OPEN ACCESS
IOP Publishing
Journal of Physics A: Mathematical and Theoretical
J. Phys. A: Math. Theor. **58** (2025) 045001 (27pp)
https://doi.org/10.1088/1751-8121/ada748

Generalised Ornstein–Uhlenbeck process: memory effects and resetting

P Trajanovski[1], P Jolakoski[1,5], L Kocarev[1,2], R Metzler[3,4,*] and T Sandev[1,5,6]

[1] Research Center for Computer Science and Information Technologies, Macedonian Academy of Sciences and Arts, Bul. Krste Misirkov 2, 1000 Skopje, Macedonia
[2] Faculty of Computer Science and Engineering, Ss. Cyril and Methodius University, PO Box 393, 1000 Skopje, Macedonia
[3] Institute of Physics and Astronomy, University of Potsdam, D-14476 Potsdam-Golm, Germany
[4] Asia Pacific Center for Theoretical Physics, Pohang 37673, Republic of Korea
[5] Institute of Physics, Faculty of Natural Sciences and Mathematics, Ss. Cyril and Methodius University, Arhimedova 3, 1000 Skopje, Macedonia
[6] Department of Physics, Korea University, Seoul 02841, Republic of Korea

E-mail: rmetzler@uni-potsdam.de

Received 6 September 2024; revised 19 December 2024
Accepted for publication 7 January 2025
Published 20 January 2025

Abstract

In this work we consider a generalised Ornstein–Uhlenbeck (O–U) process for a stochastically driven particle in an harmonic potential which is governed by a Fokker–Planck equation in the presence of a memory kernel. We analyse the probability density function, the mean and the mean squared displacement (MSD) by employing the subordination approach connecting the operational time of the process with the (generalised) laboratory time. We provide analytical results for the mean and the MSD in case of a power-law memory kernel which corresponds to the fractional O–U process. The generalised O–U process in the presence of Poissonian resetting is also investigated by using the renewal equation approach, and the nonequilibrium stationary state approached in the

* Author to whom any correspondence should be addressed.

long time limit is obtained. The analytical results are confirmed by numerical simulations based on the coupled Langevin equations.

Keywords: Ornstein–Uhlenbeck process, subordination, stochastic resetting, nonequilibrium stationary state

1. Introduction

Brownian motion, initially observed in the erratic movement of pollen granules suspended in a liquid by Robert Brown in 1827 [1], has since become a cornerstone in the understanding of stochastic processes and random motion in various scientific disciplines. This phenomenon, characterised by the seemingly random and continuous movement of particles, has played a pivotal role in shaping the theoretical and mathematical landscape of statistical physics. Albert Einstein [2] and Marian Smoluchowski [3] independently laid the foundation for the statistical treatment of Brownian motion in the early 20th century, opening the door to extensive theoretical and mathematical investigations. Paul Langevin subsequently stated an extension of Newton's second law with a fluctuating force, resulting in an ordinary stochastic differential equation. The Ornstein–Uhlenbeck (O–U) process, introduced by Leonard Ornstein [4] and George Uhlenbeck [5] emerged as a significant extension of Brownian motion, providing a more nuanced understanding of the dynamics of particles undergoing random motion in a harmonic potential. Originally, it was introduced as a model of the velocity of a Brownian particle.

The O–U process is particularly notable for its ability to describe the motion of particles subject to both random fluctuations and a restoring force, offering a valuable framework for modelling diverse phenomena ranging from physics to finance. Ornstein and Uhlenbeck's seminal work in the 1930 s not only provided an exact expression for the mean squared displacement (MSD) of harmonically bound particles but also established a profound connection between their model and the Fokker–Planck equation, contributing to the broader comprehension of the universality of Brownian motion as a Markovian phenomenon. In contemporary research, it has become evident that non-Markovian anomalous transport is a pervasive and general phenomenon across various scientific fields. This has led to the extension of the O–U approach to non-Markov random processes, garnering considerable attention. This extension encompasses non-Markovian Langevin equations [6] and the spectral properties of the Fokker–Planck equation propagator [7]. We mention that the motivation for exploring the O–U process and its generalisations lies in their broad applicability across various fields, including modelling anomalous diffusion in inhomogeneous media [8, 9], which results in fractional transport [10, 13], as well as applications in turbulent diffusion [14, 15]; moreover, to describe overdamped Brownian particles in optical tweezers [18] and tracer diffusion in critical random environments [19], financial modelling [16, 20], and the activity of neuronal systems [21]. Additionally, there is a broader connection between random matrix theory and Gaussian processes with long-range correlations [17].

The O–U process, in its standard and generalised variations, both with and without resetting, have been subject to extensive examination in previous works, as documented in [22–27]. Addressing the intricacies of the O–U process in the presence of stochastic resetting, the analysis in [23], represents a pivotal contribution to the understanding of how stochastic resetting influences its dynamics. Furthermore, the investigation of the O–U process on two and three-dimensional comb structures, with and without resetting, as discussed in [28, 29], provides insights into the process within a specific geometric context.

Building upon this established groundwork, our paper seeks to extend the O–U process by implementing a memory kernel within the corresponding Fokker–Planck equation. The paper is organised as follows. In section 2, we derive the Fokker–Planck equation with memory kernel for the generalised O–U process from the corresponding equation for the standard O–U process by using the subordination approach. We give general results for the mean and the MSD for a general form of the memory kernel. The time fractional O–U process is considered and analysed in details in section 3. The analytically obtained results are compared with the simulations which are performed by using the Langevin equation approach. In section 4 we consider the generalised O–U process under stochastic resetting by introducing exponentially truncated memory kernel. As a special case we consider the time fractional O–U process under stochastic resetting and we derive the mean and the MSD. The system approaches a non-equilibrium stationary state in the long time limit due to the resetting mechanism. The summary of the obtained results is given in section 5. In the Appendices we give the definitions and properties of the fractional integral and derivatives, as well as of different Mittag–Leffler functions, and the formulation of the Tauberian theorems. We also provide results for the mean and the MSD for a generalised O–U process with mixed power-law memory kernel, as well as for a combination of the standard and subdiffusive O–U process.

2. From standard to generalised O–U process

2.1. Standard O–U process

In this section we introduce the O–U process. We will lay out some of the main results of this process such as the probability density function (PDF), and the first two moments of the displacement as well elaborate on the main properties of the process.

The standard O–U process is defined in terms of the modified stochastic overdamped Langevin equation (see [5, 20, 30])

$$\dot{x}(t) = \lambda[\mu - x(t)] + \sigma\xi(t), \tag{1}$$

where λ is the rate of mean reversion and represents the magnitude of the drift with which the process is driven towards some long term mean value μ, $\xi(t)$ is a white noise of zero mean and correlation $\langle\xi(t)\xi(t')\rangle = \delta(t-t')$, and σ is the standard deviation. The first term of equation (1) is the deterministic or the driving part of the equation, while the second term stands for the stochastic part, contributing to the process only with the random fluctuations due to the white noise.

The standard O–U process can also be defined by its corresponding Fokker–Planck equation

$$\frac{\partial}{\partial t}P_0(x,t) = L_{\mathrm{FP}}P_0(x,t), \tag{2}$$

with initial condition $P_0(x,t=0) = \delta(x-x_0)$ and zero boundary conditions at infinity both for the PDF $P_0(x,t)$ and its first space derivative, where

$$L_{\mathrm{FP}} = \lambda\frac{\partial}{\partial x}[(x-\mu)] + \frac{\sigma^2}{2}\frac{\partial^2}{\partial x^2}, \tag{3}$$

is the Fokker–Planck operator. The solution to the partial differential equation for the O–U process (2) is given by [31]

$$P_0(x,t) = \frac{\exp\left(-\frac{\left[x-x_0\mathrm{e}^{-\lambda t}-\mu\left(1-\mathrm{e}^{-\lambda t}\right)\right]^2}{\frac{\sigma^2}{\lambda}\mathrm{e}^{-2\lambda t}\left(\mathrm{e}^{2\lambda t}-1\right)}\right)}{\sqrt{2\pi\frac{\sigma^2}{2\lambda}\mathrm{e}^{-2\lambda t}\left(\mathrm{e}^{2\lambda t}-1\right)}}. \tag{4}$$

The previous expression for the PDF is used to further calculate the moments of the displacement, namely the mean value and the MSD

$$\langle x(t)\rangle = x_0\mathrm{e}^{-\lambda t} + \mu\left(1-\mathrm{e}^{-\lambda t}\right), \tag{5}$$

$$\langle x^2(t)\rangle = x_0^2\mathrm{e}^{-2\lambda t} + \mu^2\left(1+\mathrm{e}^{-2\lambda t}\right) - 2\mu^2\mathrm{e}^{-\lambda t} + \frac{\sigma^2}{2\lambda}\left(1-\mathrm{e}^{-2\lambda t}\right) + 2\mu x_0\left(1-\mathrm{e}^{-\lambda t}\right)\mathrm{e}^{-\lambda t}. \tag{6}$$

This can also be represented as a relaxation to the thermal value, see [8]. The long-time limit of the MSD saturates at $\langle x^2(t)\rangle \sim \mu^2 + \frac{\sigma^2}{2\lambda}$ due to the potential, and for $\lambda = 0$ we retrieve the result for the MSD of the normal Wiener process $\langle x^2(t)\rangle = x_0^2 + \sigma^2 t$. We note that in Laplace space the mean value and the MSD are given by

$$\langle \hat{x}(s)\rangle = \frac{x_0}{s+\lambda} + \mu\lambda\frac{s^{-1}}{s+\lambda}, \tag{7}$$

$$\langle \hat{x}^2(s)\rangle = \frac{x_0^2+\sigma^2 s^{-1}}{s+2\lambda} + \frac{2\lambda\mu\left(x_0+\lambda\mu s^{-1}\right)}{(s+\lambda)(s+2\lambda)}, \tag{8}$$

respectively. These results will be used later for calculation of the mean and MSD in case of generalised O–U process with memory.

2.2. Generalised O–U process: subordination approach

In this section we will consider a generalisation of the standard O–U process, which is the main objective of this paper. Under these generalisations the standard and fractional O–U processes arise as special cases. Here we will use the subordination approach to calculate the displacement moments of the process, namely the mean value and the MSD. The generalised process in question mathematically can be described by considering a continuous time random walk (CTRW)[7] model according to which the PDF to find the particle at position x at time t is given by [34]

$$P(x,t) = \sum_n P_0(x,n)\,h_n(t), \tag{9}$$

where $P_0(n,t)$ is the PDF to find the particle at x after n steps for the standard O–U process, while $h_n(t)$ is the PDF to make exactly n steps up to time t. This function is connected to the waiting time PDF $\psi(t)$ in the Laplace space as [34]

$$\hat{h}_n(s) = \frac{1-\hat{\psi}(s)}{s}\hat{\psi}^n(s) \simeq \frac{\hat{\phi}(s)}{s}\mathrm{e}^{-n\hat{\phi}(s)}, \tag{10}$$

[7] In its decoupled version, a CTRW is defined as a random walk process based on a jump length PDF $\lambda(x)$ and a waiting time PDF $\psi(t)$. Here we consider a finite-variance $\lambda(x)$ and a $\psi(t)$ with both finite and infinite mean waiting time [32, 33].

where $\hat{\phi}(s) = 1 - \hat{\psi}(s)$. The random number of steps n performed in this CTRW process has the role of the operational time. The MSD is a function of the mean number of steps $\langle x^2(t)\rangle \sim \langle n(t)\rangle$.

This CTRW process in the continuum approximation can be described in terms of the coupled Langevin Equations [35–39]

$$\begin{cases} \dot{x}(u) &= \lambda[\mu - x(u)] + \sigma\xi(u), \\ \dot{t}(u) &= \zeta(u), \end{cases} \tag{11}$$

where $\lambda > 0$ and $\sigma > 0$, $\xi(u) = \frac{\mathrm{d}B(u)}{\mathrm{d}u}$ represents a white Gaussian noise with zero mean $\langle\xi(u)\rangle = 0$ and correlation $\langle\xi(u)\xi(u')\rangle = \delta(u-u')$, $B(u)$ is the standard Brownian motion, and thus the process $x(u) = \int_0^u \{\lambda[\mu - x(u')] + \sigma\xi(u')\}\,\mathrm{d}u'$ is the standard O–U process with PDF (4), while $\zeta(u)$ is a completely one-sided Lévy stable noise. The inverse process $\mathcal{S}(t)$ of the one-sided Lévy stable process $t(u)$ with the characteristic function $\left\langle \mathrm{e}^{-st(u)}\right\rangle = \mathrm{e}^{-\hat{\Psi}(s)u}$, where $\hat{\Psi}(s)$ is a 'characteristic exponent'[8], is given by $\mathcal{S}(t) = \inf\{u > 0 : t(u) > t\}$, i.e. it represents a distribution of first passage times for the operational time u given the laboratory time t [35, 42]. The processes $B(u)$ and $\mathcal{S}(t)$ are independent. From the coupled Langevin equations (11), one concludes that $x(t)$ is parametrised in terms of the number of steps u (in the CTRW model it corresponds to n), the so-called path or arc length along a particular trajectory and initially introduced in [35] and later investigated in [43–45], as an intermediate variable. The parameter u is also known as operational time. Its connection to the time variable t is given by $t(u) = \int_0^u \tau(u')\mathrm{d}u'$, where $\tau(u)$ is the total of individual waiting times τ for each step. The path or arc length u can also be explained as steps or 'eigentime' of coupled filtering process governed by a specific distribution, which is in control of the waiting times of the main process. The corresponding Fokker–Planck equation for the process is

$$\frac{\partial}{\partial t}P(x,t) = \frac{\mathrm{d}}{\mathrm{d}t}\int_0^t \eta(t-t')\left\{\lambda\frac{\partial}{\partial x}\left[(x-\mu)P(x,t')\right] + \frac{\sigma^2}{2}\frac{\partial^2}{\partial x^2}P(x,t')\right\}\mathrm{d}t', \tag{12}$$

where $\eta(t) = \mathcal{L}^{-1}\left[1/\hat{\Psi}(s)\right]$ is a memory kernel, which is connected to the waiting time PDF in the CTRW model as $\hat{\psi}(s) \sim 1 - 1/\hat{\eta}(s)$ [34]. The memory kernel is such that $\lim_{s\to 0}\frac{1}{\hat{\eta}(s)} = 0$, as well as $\frac{1}{\hat{\eta}(s)}$ is a complete Bernstein function which is needed for preserving the non-negativity of the solution of the generalised Fokker–Planck equation, see for example [46–49]. This equation contains many limiting cases. For example, for $\eta(t) = 1$ we recover the standard O–U process given with equation (2), while for $\lambda = 0$, equation (12) is reduced to the generalised diffusion equation for subordinated Brownian motion [34, 46, 47].

We can find the solution of the generalised Fokker–Planck equation (12) by using the subordination approach [50–54], i.e. by the subordination integral

$$P(x,t) = \int_0^\infty P_0(x,u)\,h(u,t)\,\mathrm{d}u, \tag{13}$$

[8] Note that for $\hat{\Psi}(s) = s^\alpha$, $0 < \alpha < 1$, the noise $\zeta(u)$ is one-sided α-stable Lévy noise with the stable index $0 < \alpha < 1$, while $\mathcal{S}(t)$ is called the inverse-time α-stable subordinator [40, 41].

which follows from the PDF obtained from the CTRW model (9) ($n \to u$, $h_n(t) \to h(u,t)$ and $\sum_n \to \int \mathrm{d}u$). In the Laplace space it becomes

$$\begin{aligned}\hat{P}(x,s) &= \int_0^\infty P_0(x,u)\,\hat{h}(u,s)\,\mathrm{d}u \\ &= \int_0^\infty P_0(x,u)\,\frac{1}{s\hat{\eta}(s)}\mathrm{e}^{-u/\hat{\eta}(s)}\mathrm{d}u = \frac{1}{s\hat{\eta}(s)}\hat{P}_0\left(x,\frac{1}{\hat{\eta}(s)}\right),\end{aligned} \tag{14}$$

where $P_0(x,t)$ is the solution of the Fokker–Planck equation for standard O–U process (4) (without memory kernel, i.e. $\eta(t)=1$), and the subordination function $h(u,t)$ in Laplace space is given by

$$\hat{h}(u,s) = \frac{1}{s\hat{\eta}(s)}\mathrm{e}^{-u/\hat{\eta}(s)}. \tag{15}$$

From equation (14) one can easily calculate the mean $\langle x(t)\rangle_{\mathrm{g}} = \int_{-\infty}^{\infty} xP(x,t)\,\mathrm{d}x$ and the MSD $\langle x^2(t)\rangle_{\mathrm{g}} = \int_{-\infty}^{\infty} x^2P(x,t)\,\mathrm{d}x$ for the generalised O–U process. Therefore, in Laplace space, we have

$$\langle\hat{x}(s)\rangle_{\mathrm{g}} = \int_{-\infty}^{\infty} x\hat{P}(x,s)\,\mathrm{d}x = \frac{1}{s\hat{\eta}(s)}\int_{-\infty}^{\infty} x\hat{P}_0\left(x,\frac{1}{\hat{\eta}(s)}\right)\mathrm{d}x = \frac{1}{s\hat{\eta}(s)}\langle\hat{x}(1/\hat{\eta}(s))\rangle, \tag{16}$$

$$\langle\hat{x}^2(s)\rangle_{\mathrm{g}} = \int_{-\infty}^{\infty} x^2\hat{P}(x,s)\,\mathrm{d}x = \frac{1}{s\hat{\eta}(s)}\int_{-\infty}^{\infty} x^2\hat{P}_0\left(x,\frac{1}{\hat{\eta}(s)}\right)\mathrm{d}x = \frac{1}{s\hat{\eta}(s)}\langle\hat{x}^2(1/\hat{\eta}(s))\rangle, \tag{17}$$

respectively. From here one can conclude that the mean $\langle\hat{x}(t)\rangle_{\mathrm{g}}$ and the MSD $\langle\hat{x}^2(t)\rangle_{\mathrm{g}}$ of the generalised O–U process for a specific form of the memory kernel can be found explicitly in Laplace space from the corresponding mean $\langle\hat{x}(s)\rangle$, see equation (7), and the MSD $\langle\hat{x}^2(s)\rangle$, see equation (8), for the standard O–U process. By using relations (7) and (16) for the mean, and relations (8) and (17) for the MSD, we finally find

$$\langle\hat{x}(s)\rangle_{\mathrm{g}} = \frac{[x_0+\lambda\mu\hat{\eta}(s)]\,s^{-1}}{1+\lambda\hat{\eta}(s)}, \tag{18}$$

$$\langle\hat{x}^2(s)\rangle_{\mathrm{g}} = \frac{\left[x_0^2+\sigma^2\hat{\eta}(s)\right]s^{-1}}{1+2\lambda\hat{\eta}(s)} + \frac{2\lambda\mu\,[x_0+\lambda\mu\hat{\eta}(s)]\,s^{-1}\hat{\eta}(s)}{[1+2\lambda\hat{\eta}(s)]\,[1+\lambda\hat{\eta}(s)]}. \tag{19}$$

For the case $\mu=0$, these results reduce to

$$\langle\hat{x}(s)\rangle_{\mathrm{g}} = \frac{x_0}{s\,[1+\lambda\hat{\eta}(s)]}, \tag{20}$$

and

$$\langle\hat{x}^2(s)\rangle_{\mathrm{g}} = \frac{\left[x_0^2+\sigma^2\hat{\eta}(s)\right]s^{-1}}{1+2\lambda\hat{\eta}(s)}. \tag{21}$$

Here we note that if instead of the harmonic potential, we consider a constant external force, one can show that the generalised fluctuation–dissipation theorem is satisfied, as in the case of the corresponding process without memory kernel, see [9, 55].

Remark 1. The same results for the mean and the MSD can be obtained from the Fokker–Planck equation (12). Even though there is no exact solution of the Fokker–Planck equation (12), one can find exact expressions for the moments of the PDF. In order to obtain

the explicit expressions for these moments, equation (12) is multiplied by x and x^2 correspondingly and integrated from $-\infty$ to $+\infty$. Following these steps the equation for the mean value is

$$\frac{\partial}{\partial t}\langle x(t)\rangle_{\mathrm{g}} = \frac{\mathrm{d}}{\mathrm{d}t}\int_0^t \eta(t-t')\left[\lambda\langle x(t')\rangle_{\mathrm{g}} - 2\lambda\langle x(t')\rangle_{\mathrm{g}} - \lambda\mu\right]\mathrm{d}t', \tag{22}$$

and in Laplace space

$$s\langle\hat{x}(s)\rangle_{\mathrm{g}} - x_0 = s\hat{\eta}(s)\left[-\lambda\langle\hat{x}(s)\rangle_{\mathrm{g}} - \frac{\lambda\mu}{s}\right]. \tag{23}$$

From here one finds relation (18). Now performing the same steps for the MSD we end up with the equation

$$\frac{\partial}{\partial t}\langle x^2(t)\rangle_{\mathrm{g}} = \frac{\mathrm{d}}{\mathrm{d}t}\int_0^t \eta(t-t')\times\left[-2\lambda\langle x^2(t')\rangle_{\mathrm{g}} + 2\lambda\mu\langle x(t')\rangle + \sigma^2\right]\mathrm{d}t', \tag{24}$$

or in Laplace space

$$s\langle\hat{x}^2(s)\rangle_{\mathrm{g}} - x_0^2 = s\hat{\eta}(s)\left[-2\lambda\langle\hat{x}^2(s)\rangle_{\mathrm{g}} + 2\lambda\mu\langle\hat{x}(s)\rangle_{\mathrm{g}} + \frac{\sigma^2}{s}\right], \tag{25}$$

from where we derive relation (19).

3. Power-law memory kernel: time fractional O–U process

Now let us examine different memory kernels that can be employed in the generalised Fokker–Planck equation (12) and the corresponding equations for the mean value (18) and the MSD (19). First, we will investigate the process by implementing the power-law memory kernel $\eta(t) = \frac{t^{\alpha-1}}{\Gamma(\alpha)}$, $0<\alpha<1$, $\hat{\eta}(s) = s^{-\alpha}$, which corresponds to the fractional O–U process governed by (see [8, 9] for $\mu = 0$)

$$\frac{\partial}{\partial t}P(x,t) = {}_{\mathrm{RL}}D_t^{1-\alpha}\left\{\lambda\frac{\partial}{\partial x}\left[(x-\mu)P(x,t')\right] + \frac{\sigma^2}{2}\frac{\partial^2}{\partial x^2}P(x,t')\right\}, \tag{26}$$

where ${}_{\mathrm{RL}}D_t^{1-\alpha}$ is the Riemann–Liouville fractional derivative (A.3) of order $0<1-\alpha<1$. We introduce such a memory kernel with $0<\alpha<1$ since $\hat{\Psi}(s) = \frac{1}{\hat{\eta}(s)} = s^{\alpha}$, which means that the noise $\zeta(u)$ is one-sided α-stable Lévy noise with stable index $0<\alpha<1$. This case relates to the long-tailed waiting time PDF of the form $\psi(t)\sim t^{-\alpha-1}$ in the CTRW model, see [34]. We note that the PDF of this equation for $\mu = 0$ was obtained as a series of Hermite polynomials and via a subordination integral in [8, 9].

3.1. Mean value and MSD

From the general results for the mean (18) and the MSD (19), for the power-law memory kernel we have

$$\langle\hat{x}(s)\rangle_{\mathrm{g}} = \frac{(x_0 + \lambda\mu s^{-\alpha})s^{\alpha-1}}{s^{\alpha}+\lambda}, \tag{27}$$

$$\langle \hat{x}^2(s)\rangle_{\rm g} = \frac{\left(x_0^2+\sigma^2 s^{-\alpha}\right)s^{\alpha-1}}{s^\alpha+2\lambda} + \frac{2\lambda\mu\left(x_0+\lambda\mu s^{-\alpha}\right)s^{\alpha-1}}{\left(s^\alpha+2\lambda\right)\left(s^\alpha+\lambda\right)}, \tag{28}$$

which by inverse Laplace transform become

$$\langle x^2(t)\rangle_{\rm g} = x_0^2 E_\alpha\left(-2\lambda t^\alpha\right) + \sigma^2 t^\alpha E_{\alpha,\alpha+1}\left(-2\lambda t^\alpha\right) + 2\lambda\mu x_0 t^\alpha E_{(\alpha,2\alpha),\alpha+1}\left(-3\lambda t^\alpha, -2\lambda^2 t^{2\alpha}\right) + 2\lambda^2\mu^2 t^{2\alpha} E_{(\alpha,2\alpha),2\alpha+1}\left(-3\lambda t^\alpha, -2\lambda^2 t^{2\alpha}\right). \tag{29}$$

Here $E_\alpha(z)$, $E_{\alpha,\beta}(z)$, and $E_{(\alpha_1,\alpha_2,\ldots,\alpha_n),\beta}(z_1,z_2,\ldots,z_n)$ are one parameter (A.9), two parameter (A.8) and multinomial (A.13) Mittag–Leffler functions, respectively. By using the Tauberian theorems, see appendix B, one can find that in the long time limit the mean value μ is approached,

$$\langle x(t)\rangle_{\rm g} \sim \frac{x_0}{\lambda}\frac{t^{-\alpha}}{\Gamma(1-\alpha)}\left[1-\frac{\Gamma(1-\alpha)t^{-\alpha}}{\lambda\Gamma(1-2\alpha)}\right] + \mu\left[1-\frac{1}{\lambda\Gamma(1-\alpha)}t^{-\alpha}\right], \tag{30}$$

and the MSD approaches to the thermal equilibrium $\langle x_{\rm th}^2\rangle = \frac{\sigma^2}{2\lambda}+\mu^2$,

$$\langle x^2(t)\rangle_{\rm g} \sim \frac{x_0^2}{2\lambda}\frac{t^{-\alpha}}{\Gamma(1-\alpha)}\left[1-\frac{\Gamma(1-\alpha)t^{-\alpha}}{2\lambda\Gamma(1-2\alpha)}\right] + \frac{\sigma^2}{2\lambda}\left[1-\frac{t^{-\alpha}}{2\lambda\Gamma(1-\alpha)}\right] + \frac{\mu x_0}{\lambda}\frac{t^{-\alpha}}{\Gamma(1-\alpha)}\left[1-\frac{3\Gamma(1-\alpha)t^{-\alpha}}{\lambda\Gamma(1-2\alpha)}\right] + \mu^2\left[1-\frac{3}{2\lambda}\frac{t^{-\alpha}}{\Gamma(1-\alpha)}\right]. \tag{31}$$

For the special case with $\mu=0$, we recover the following result for the mean [8, 9]

$$\langle x(t)\rangle_{\rm g} = x_0 E_\alpha\left(-\lambda t^\alpha\right), \tag{32}$$

and for the MSD [8, 9]

$$\langle x^2(t)\rangle_{\rm g} = x_0^2 E_\alpha\left(-2\lambda t^\alpha\right) + \sigma^2 t^\alpha E_{\alpha,\alpha+1}\left(-2\lambda t^\alpha\right). \tag{33}$$

In the long time limit the MSD relaxes to the thermal equilibrium $\langle x_{\rm th}^2\rangle = \frac{\sigma^2}{2\lambda}$ [9] exponentially for $\alpha=1$ and as a power-law for $0<\alpha<1$. This power-law approach is expected due to the long-tailed waiting time PDF $\psi(t)\sim t^{-\alpha-1}$, $0<\alpha<1$, which results in the emergence of a Mittag–Leffler relaxation[9] instead of the exponential relaxation in the standard O–U process. For $\lambda=0$ the MSD becomes $\langle x^2(t)\rangle_{\rm g} = x_0^2+\sigma^2\frac{t^\alpha}{\Gamma(1+\alpha)}$, as it should be, since it is the MSD for anomalous diffusive process, obtained from CTRW theory for long-tailed waiting time PDF $\psi(t)\sim t^{-\alpha-1}$, $0<\alpha<1$. We note that the case with $\alpha=1/2$ corresponds to the O–U process along the backbone of the two dimensional comb, which consists of a main channel in x-direction (so-called backbone) and side branches in y-direction (so-called fingers of the comb) in which the particle can be stacked with a power-law waiting time $\psi(t)\sim t^{-3/2}$ [28], while the case with $\alpha=1/4$ to the O–U process along the backbone of the three dimensional comb, which consist of a main channel along the x-direction, side branches in y-direction and secondary branches in z-direction [29].

[9] In the long time limit the Mittag–Leffler function asymptotically behaves as a power-law, see (A.12).

3.2. Langevin equation approach

The method for Monte Carlo simulations for this particular problem, when we have a generalised power law exponent α is not the same as the method used for simulating anomalous diffusion of a particle on a comb structure investigated in [28, 29, 56–59], even though as previously mentioned, certain values of the exponent ($\alpha = 1/2, 1/4$) recreate the same results as the anomalous diffusion on two dimensional and three dimensional comb structures, respectively. The procedure used for simulating the problem of interest in this paper, namely, the O–U process with a memory kernel is given in detail in [45]. The equations used to simulate the processes are

$$x(s) = x(0) + \int_0^s F(x(s'))\,\mathrm{d}s' + \int_0^s \mathrm{d}W(x(s'))\,, \tag{34}$$

and

$$t(s) = t(0) + \int_0^s \mathrm{d}L_\alpha(s')\,, \tag{35}$$

where $\mathrm{d}W$ and $\mathrm{d}L_\alpha$ are the infinitesimal increments of Wiener and one-sided α-stable Lévy processes, respectively. For the purpose of simulating the process these equations have to be discretised with suitable discrete increment Δs. The discretised equations are given as

$$x(s+\Delta s) = x(s) + \Delta s F(x(s)) + \eta(s,\Delta s)\,, \tag{36}$$

and

$$t(s+\Delta s) = t(s) + \tau_\alpha(s+\Delta s)\,. \tag{37}$$

The random variables $\eta(s_i,\Delta s_i)$ have to be drawn from a Gaussian PDF with variance $\sigma^2 = \Delta s$, and the variables $\tau_\alpha(s_i,\Delta s_i)$ have to comply with a distribution of the form $\frac{1}{\Delta s^\alpha} L_\alpha\left(\frac{\tau_\alpha}{\Delta s^\alpha}\right)$ defined as [45],

$$L_\alpha(x) = \frac{1}{\pi}\Re\left\{\int_0^\infty \exp\left(-\mathrm{i}kz - z^\alpha \exp\left(-\mathrm{i}\frac{\alpha\pi}{2}\right)\right)\mathrm{d}z\right\} \tag{38}$$

The generation of the random numbers $\tau_\alpha(s_i,\Delta s_i)$ for the case of $0 < \alpha \leq 1$ can efficiently can be done by taking the form [45]

$$\tau_\alpha(s_i,\Delta s_i) = (\Delta s)^{\frac{1}{\alpha}} \frac{\sin(\alpha[V_i+\pi/2])}{[\cos(V_i)]^{1/\alpha}} \times \left\{\frac{\cos(V_i - \alpha[V_i+\pi/2])}{W_i}\right\}^{\frac{1-\alpha}{\alpha}}, \tag{39}$$

where $V_i = \pi(u_i^1 - 1/2)$ is a random variable uniformly distributed on $[-\pi/2, +\pi/2]$, and $W_i = -\log(u_i^2)$ is a random variable with mean 1, and $u_i^{1,2}$ are independent variables that are uniformly distributed on the interval [0,1]. In the case when $\alpha = 1$, $\tau_1(s_i,\Delta s_i) = \Delta s$ is retrieved.

Figure 1 shows trajectories of the O–U process with power-law memory kernel for different exponents α. The solid lines correspond to the process $x(t)$, while the dashed lines correspond to $s(t)$, namely the inverse process of $t(s)$, for details see [45]. As is clearly visible from the trajectories, the scaling exponent α of the waiting time PDF plays a crucial role in the particle dynamics. While for all $0 < \alpha < 1$ the characteristic waiting time diverges, smaller values of

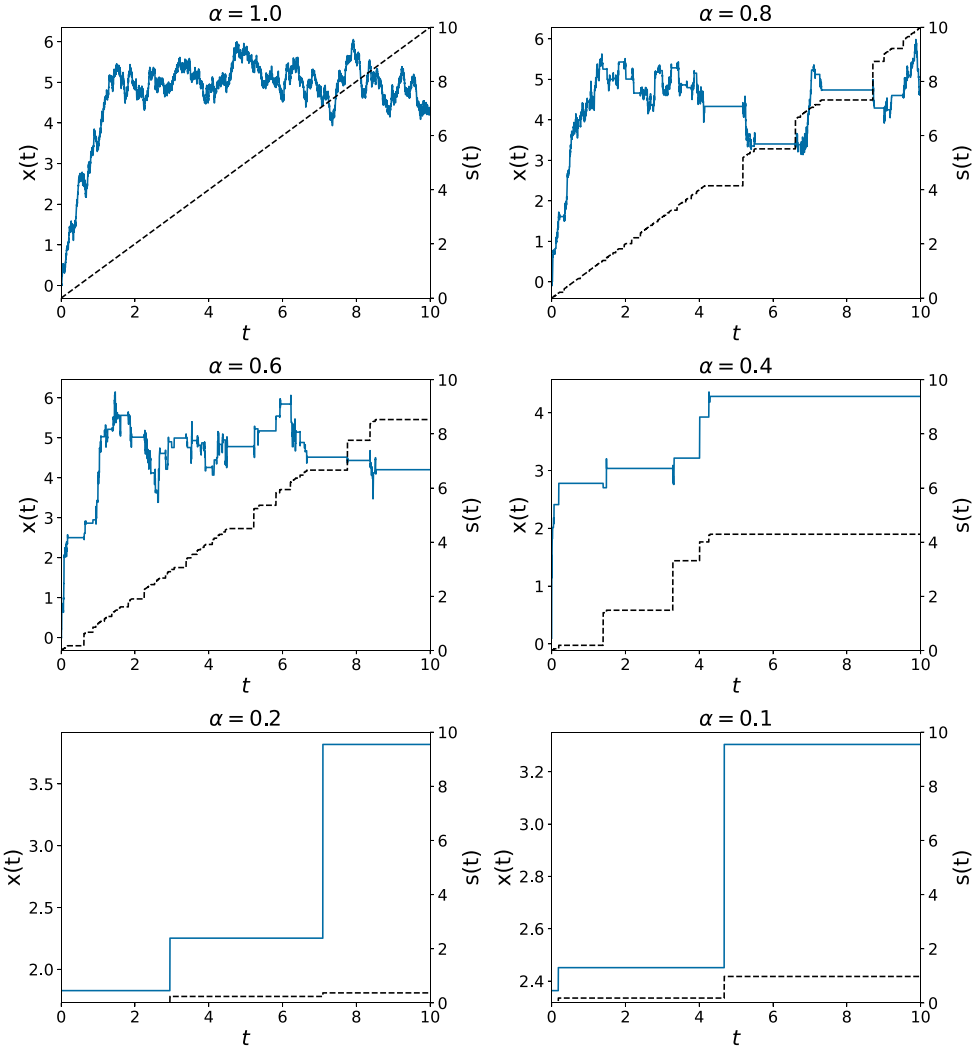

Figure 1. Typical trajectories of the subordinated O–U process for different α. The solid blue lines correspond to the process $x(t)$, while the dashed black lines to the process $s(t)$. We set $\mathrm{d}t = 0.001$, $\mathrm{d}s = 0.0001$, $\mu = 5$, $\lambda = 1$ and $\sigma = 1$.

α mean that the waiting time PDF has an even shallower tail and thus allows, typically, for even longer waiting times. The progress in space for a particle with smaller α is thus slower, as already anticipated by the α-dependence of the MSD. Namely, by lowering the exponent below unity, the process experiences scale-free waiting times, in doing so delaying the particle from reaching the long-term mean value μ. The smaller the value of the exponent, the longer these waiting times become, and the relaxation to the long-term mean value is a power-law. The same can be concluded from the calculation of the MSDs of the process for different exponents as shown in figure 2. Given that the O–U process is stationary, we see an early

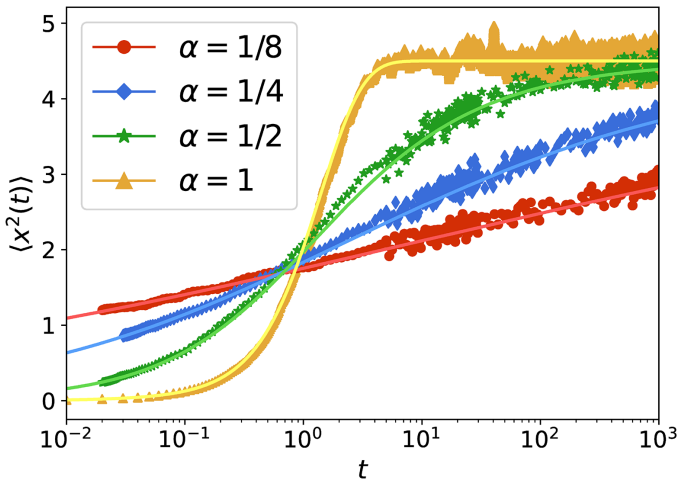

Figure 2. MSD (29) (solid lines) and MSD obtained by simulations (36) and (37) (markers) for the O–U process with power-law memory kernel $\eta(t) = \frac{t^{\alpha-1}}{\Gamma(\alpha)}$, $\hat{\eta}(s) = s^{-\alpha}$. We set $x_0 = 0$, $\sigma = 1$, $\lambda = 1$, $\mu = 2$, $\mathrm{d}t = 0.01$, $\mathrm{d}s = 0.001$, $T = 1000$ and $N = 1000$.

and rapid saturation of the process when we have the standard process and normal diffusion, which occurs when the value of the exponent $\alpha = 1$, due to the exponential relaxation. This is not the case when anomalous diffusion ($\alpha < 1$) is present, where in order for the process to reach the characteristic saturation of the O–U process a long time has to pass. In other words, as the exponent value decreases, the speed of reaching the long-term mean value μ decreases as well.

In figure 2 we see a good agreement between the analytical results for the MSDs (29) and the simulations of the process, even though simulating the time fractional O–U process is not a trivial task. From the simulations of the MSDs, see figure 2, we can conclude that the results are more robust and precise for larger exponent values α and longer times t. To plot the analytical results for the MSD as function of time t, we apply the numerical inverse Laplace transform package in Wolfram Mathematica [60–62] to the MSD (28) in Laplace space.

In figure 3 we illustrate the numerical calculations of the PDFs $P(x,t)$ that give the solution to the fractional differential equation (26) (solid lines) and the corresponding simulations for different values of the exponent α in the long-time limit ($t = 10^4$). The numerical solution of the fractional Fokker–Planck equation (26) uses the numerical package for solving fractional partial differential equations in Wolfram Mathematica [63]. Again, it is evident here that the exponent α is a crucial factor for determining the speed of the evolution of the system through time. For smaller exponents α the particle has a larger probability to be found around its initial position even as the process progresses through time, which is a consequence of the large waiting times as is visible from the trajectories even though the O–U process is driven towards some long-term value μ. In figure 4 we give the time evolution of the PDF for different values of α. Here, clear cusps at the initial positions are visible. These cusps are more evident for smaller exponents α, when the diffusion of the particles is slower, and particles stay around the initial position longer, therefore exhibiting this cusp-like behaviour of the PDF in the initial position. These cusps are investigated to great extent in [64, 65]. In appendix C, we investigate

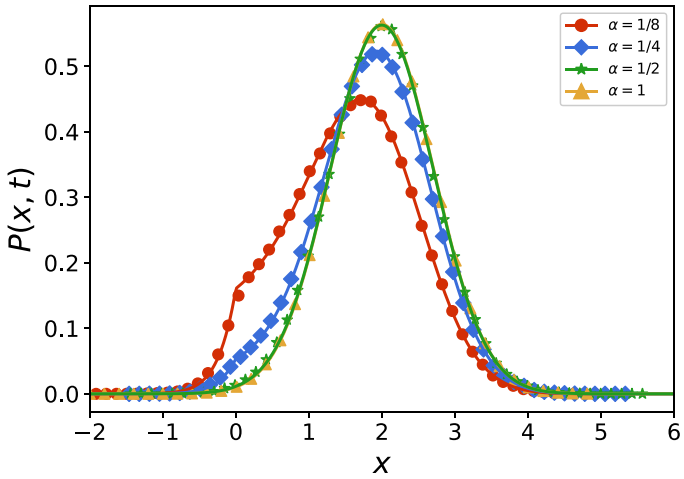

Figure 3. Long time behaviour of the solution $P(x,t)$ of equation (26) with a power-law memory kernel $\eta(t) = \frac{t^{\alpha-1}}{\Gamma(\alpha)}$, $\hat{\eta}(s) = s^{-\alpha}$, for different values of α; numerical solutions (solid lines), simulations (markers). We set $x_0 = 0$, $\mu = 2$, $\sigma = 1$, $\lambda = 1$, $N = 10^5$ and $t = 10^4$.

mixed fractional O–U process, characterised by two fractional exponents. As a special case we recover the results for a combination of fractional and standard O–U processes. The exact analytical expressions for the mean and the MSD are given, and the graphical representation of the MSD for different values of the fractional exponents is shown in figure C1.

In appendix D, we perform an error analysis between the numerical results for the PDFs and the corresponding simulations, in order to investigate the agreement between them. From (D1), we can conclude that satisfactory agreement is achieved for a statistical ensemble of $N \approx 1000$ trajectories. With further increase in the number of trajectories, we see improvement in the agreement between the numerical results and simulations but not by a significant margin.

4. Generalised O–U process with resetting

Let us now consider the exponentially truncated memory kernel

$$\eta_r(t) = \mathrm{e}^{-rt}\eta(t) \quad \rightarrow \quad \hat{\eta}_r(s) = \hat{\eta}(s+r), \tag{40}$$

with truncation rate r, where $\eta(t)$ is the same memory kernel as used before in the Fokker–Planck equation (12). We can show that for such a memory kernel the corresponding Fokker–Planck equation for the PDF

$$\frac{\partial}{\partial t}P_r(x,t) = \frac{\mathrm{d}}{\mathrm{d}t}\int_0^t \mathrm{e}^{-r(t-t')}\eta(t-t')\left\{\lambda\frac{\partial}{\partial x}\left[(x-\mu)P_r(x,t')\right] + \frac{\sigma^2}{2}\frac{\partial^2}{\partial x^2}P_r(x,t')\right\}\mathrm{d}t', \tag{41}$$

can be rewritten in the renewal form [56, 57, 66–69]

$$P_r(x,t) = \mathrm{e}^{-rt}P(x,t) + \int_0^t r\mathrm{e}^{-rt'}P(x,t')\,\mathrm{d}t', \tag{42}$$

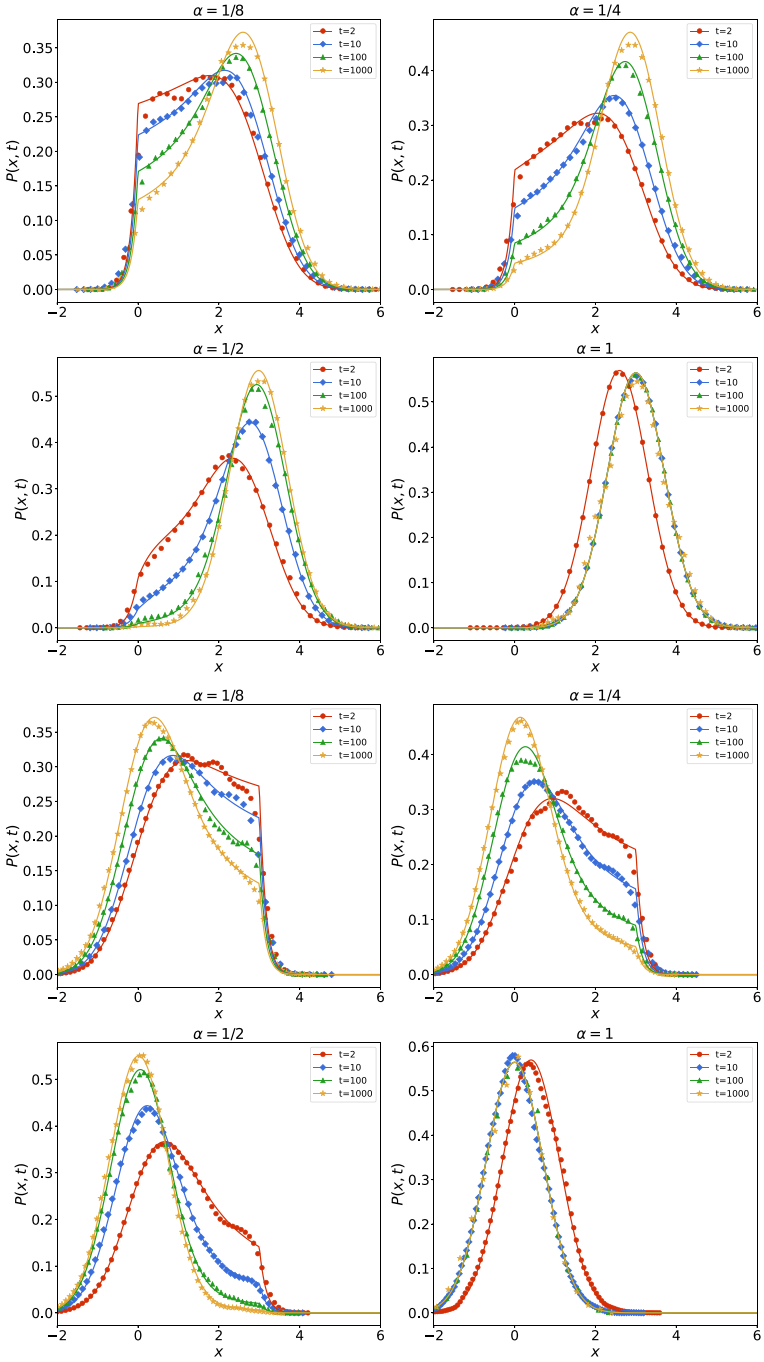

Figure 4. Time evolution of the solution $P(x,t)$ of equation (26), with a power-law memory kernel $\eta(t) = \frac{t^{\alpha-1}}{\Gamma(\alpha)}$, $0 < \alpha < 1$; numerical solutions (solid lines), simulations (markers). We set $\sigma = 1$, $\lambda = 1$, and $x_0 = 0$, $\mu = 3$ (top four plots), and $x_0 = 3$, $\mu = 0$ (bottom four plots) for $\alpha = \{1/8, 1/4, 1/2, 1\}$.

where $P(x,t)$ is the solution of the Fokker–Planck equation (12). This means that the Fokker–Planck equation (41) describes a generalised O–U process under uniform Poissonian (exponential) resetting, where the truncation rate r has the role of the resetting rate. From equation (42), by Laplace transform, one finds

$$\hat{P}_r(x,s) = \frac{s+r}{s}\hat{P}(x,s+r). \tag{43}$$

The same renewal form can be written for the MSD, i.e.

$$\langle x^2(t)\rangle_r = \mathrm{e}^{-rt}\langle x^2(t)\rangle_{\mathrm{g}} + \int_0^t r\mathrm{e}^{-rt'}\langle x^2(t')\rangle_{\mathrm{g}}\,\mathrm{d}t', \tag{44}$$

and respectively

$$\langle \hat{x}^2(s)\rangle_r = \frac{s+r}{s}\langle \hat{x}^2(s+r)\rangle_{\mathrm{g}}, \tag{45}$$

where $\langle \hat{x}^2(s)\rangle_{\mathrm{g}}$ is given by equation (19).

In the long time limit the system approaches a nonequilibrium stationary state (NESS)

$$P_r^{st}(x) = \lim_{t\to\infty} P_r(x,t) = \lim_{s\to 0} s\hat{P}_r(x,s) = r\hat{P}(x,r), \tag{46}$$

and the MSD saturates to

$$\begin{aligned}\langle x^2(t)\rangle_r &= \lim_{s\to 0} s\langle \hat{x}^2(s)\rangle_r = r\langle \hat{x}^2(r)\rangle_{\mathrm{g}} \\ &= \frac{\left[x_0^2+\sigma^2\hat{\eta}(r)\right]}{1+2\lambda\hat{\eta}(r)} + \frac{2\lambda\mu\left[x_0+\lambda\mu\hat{\eta}(r)\right]\hat{\eta}(r)}{\left[1+2\lambda\hat{\eta}(r)\right]\left[1+\lambda\hat{\eta}(r)\right]}.\end{aligned} \tag{47}$$

4.1. Fractional O–U process under resetting

Now let us investigate the case when we have uniform stochastic Poissonian resetting [70] and anomalous diffusion present in the system. The form of the memory kernel, that corresponds to that behaviour is the truncated (or tempered) power-law memory kernel $\eta_r(t) = \mathrm{e}^{-rt}\frac{t^{\alpha-1}}{\Gamma(\alpha)}$, $0<\alpha<1$, $r>0$, i.e. $\hat{\eta}_r(s) = (s+r)^{-\alpha}$, where, as we showed before, r has the role of a resetting rate. If we put the memory kernel in equation (12) we end up with the following Fokker–Planck equation

$$\frac{\partial}{\partial t}P_r(x,t) = {}_{\mathrm{TRL}}D_{0+}^{\alpha}\left\{\lambda\frac{\partial}{\partial x}\left[(x-\mu)P_r(x,t')\right] + \frac{\sigma^2}{2}\frac{\partial^2}{\partial x^2}P_r(x,t')\right\}, \tag{48}$$

where ${}_{\mathrm{TRL}}D_{0+}^{\mu}f(t)$ is the tempered R–L fractional derivative (A.5). We note that for $\alpha=1$ we recover the results for the standard O–U process under stochastic resetting.

To obtain the PDF of the fractional O–U process under resetting, we use the renewal equation in Laplace space (43), in which the PDF $\hat{P}(x,s)$ without resetting can be found from the subordination approach (14) for a power-law memory kernel with $\hat{\eta}(s) = s^{-\alpha}$. Therefore, from equation (14), the PDF without resetting reads

$$\hat{P}(x,s) = s^{\alpha-1}\hat{P}_0(x,s^{\alpha}). \tag{49}$$

while for the PDF in presence of resetting, from equation (43), we obtain

$$\hat{P}_r(x,s) = \frac{(s+r)^{\alpha}}{s}\hat{P}_0\left(x,(s+r)^{\alpha}\right). \tag{50}$$

In the same way, for the MSD in Laplace space we find

$$\begin{aligned}\langle\hat{x}^2(s)\rangle_r &= \frac{s+r}{s}\langle\hat{x}^2(s+r)\rangle_{\mathrm{g}} \\ &= \frac{s+r}{s}\left\{\frac{\left[x_0^2+\sigma^2(s+r)^{-\alpha}\right](s+r)^{\alpha-1}}{(s+r)^{\alpha}+2\lambda} + \frac{2\lambda\mu\left[x_0+\lambda\mu(s+r)^{-\alpha}\right](s+r)^{\alpha-1}}{\left[(s+r)^{\alpha}+2\lambda\right]\left[(s+r)^{\alpha}+\lambda\right]}\right\},\end{aligned} \tag{51}$$

from where one can find the exact result in terms of the three parameter (A.6) and multinomial Mittag–Leffler functions (A.13). Thus, by knowing the MSD in the absence of resetting, one can directly analyse the MSD in the presence of resetting. By inverse Laplace transform to equation (51), we find

$$\begin{aligned}\langle x^2(t)\rangle_r =& x_0^2\sum_{k=0}^{\infty}(2\lambda)^k t^{\alpha k}E_{1,\alpha k+1}^{\alpha k}(-rt) \\ &+\sigma^2\int_0^t\sum_{k=0}^{\infty}(2\lambda)^k t'^{\alpha k}E_{1,\alpha k+1}^{\alpha k}(-rt')\,(t-t')^{\alpha-1}E_{1-\alpha}^{\alpha}(-r[t-t']) \\ &+2\lambda\mu x_0\sum_{k=0}^{\infty}\sum_{l=0}^{\infty}\left(-2\lambda^2\right)^k(3\lambda)^l\binom{k+l}{l}t^{\alpha+2\alpha k+\alpha l}E_{1,\alpha+1+2\alpha k+\alpha l}^{\alpha+2\alpha k+\alpha l}(-rt) \\ &+2\lambda^2\mu^2\sum_{k=0}^{\infty}\sum_{l=0}^{\infty}\left(-2\lambda^2\right)^k(3\lambda)^l\binom{k+l}{l}t^{2\alpha+2\alpha k+\alpha l}E_{1,2\alpha+1+2\alpha k+\alpha l}^{2\alpha+2\alpha k+\alpha l}(-rt),\end{aligned} \tag{52}$$

where the geometric and binomial series formulas are used for calculating the last two terms. In the long time limit the system approaches a NESS and the MSD saturates to

$$\langle x^2(t)\rangle_r = r\langle\hat{x}_g^2(r)\rangle \sim \frac{x_0^2r^{\alpha}+\sigma^2}{r^{\alpha}+2\lambda} + \frac{2\lambda\mu\left(x_0r^{\alpha}+\lambda\mu\right)}{\left(r^{\alpha}+2\lambda\right)\left(r^{\alpha}+\lambda\right)}. \tag{53}$$

Here, by using the exponentially truncated power-law memory kernel with certain values for the anomalous exponent α we can recover the results for the O–U processes on two and three dimensional comb structures under resetting. Namely the value of the exponent $\alpha = 1/2$ recovers the results for the O–U process on the backbone of a two dimensional comb structure, see [28] and the O–U process in the main fingers on a three dimensional comb structure, see [29], and for $\alpha = 1/4$ we recover the results for the O–U process in the backbone of a three dimensional comb.

In figure 5 we present the numerical results for the MSDs of the fractional O–U process under resetting (52) for different exponents α and resetting rates r (for plotting the multinomial Mittag–Leffler functions see [71]). We can distinguish three specific cases here; namely $r < \lambda$,

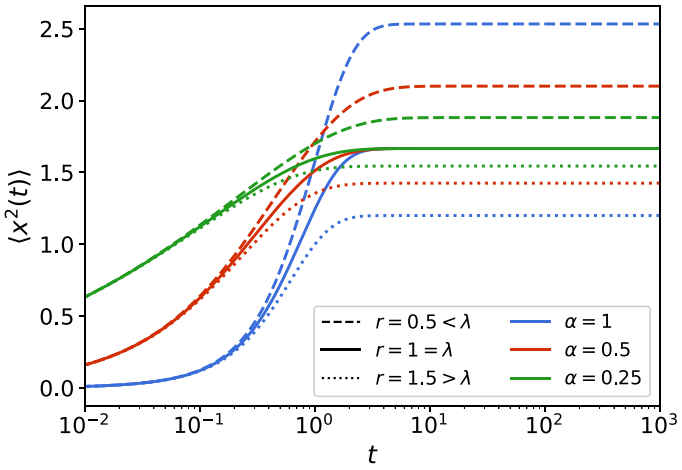

Figure 5. MSD (52) for the subdiffusive O–U process with resetting, which corresponds to the process with $\eta(t) = \mathrm{e}^{-rt}\frac{t^{\alpha-1}}{\Gamma(\alpha)}$, $r > 0$. We set $x_0 = 0$, $\mu = 2$, $\sigma = 1$ and $\lambda = 1$.

$r = \lambda$ and $r > \lambda$. From figure 5 we conclude that there is different behaviour for these three cases. When $r < \lambda$ the particles under normal diffusion, corresponding to $\alpha = 1$ have greater diffusivity than the ones undergoing anomalous diffusion $\alpha < 1$ and so the MSD for the normal diffusion is larger than for the subdiffusive one. When the resetting rate r and the mean-reverting rate λ have the same value, the two opposing processes with equal intensity produce interesting effects on the diffusivity of the particles, making the subdiffusivity of the process obsolete, meaning, the MSDs for the normal and anomalous diffusion have the same value and the waiting times have no effect on the overall diffusivity of the particle. Conversely when the resetting rate is greater than the mean-reverting rate we have the opposite effect, where particles undergoing anomalous diffusion on average reach greater distances than the ones with normal diffusion. This effect can be used in systems when intensive, frequent stochastic resetting is present and there is the need to maximise the diffusivity of the process, applying the same waiting times to the process, as in the case of diffusion on a comb structure. Here the value of the long-term mean value μ does not affect the behaviour for the three cases. If we compare the numerical results for the PDF for the fractional O–U process under resetting in figure 6 and the PDF without resetting in figure 4, the effect of stochastic resetting on the distribution is clearly evident (there is a clear cusp at the initial position), as it increases the probability of the particle being located near the initial position, which at the same time is the position where the particles are being reset to. In figure 7, the PDFs for different resetting rates r are shown, from where it is evident that with the increase in r, the localisation of the PDF around the long-term mean value μ is decreasing. This points at opposite effects of the stochastic resetting and the mean reversion of the O–U process.

5. Summary

We investigated extension of the standard O–U process based on subordination. We derived the corresponding Fokker–Planck equation starting from the one for the standard O–U process,

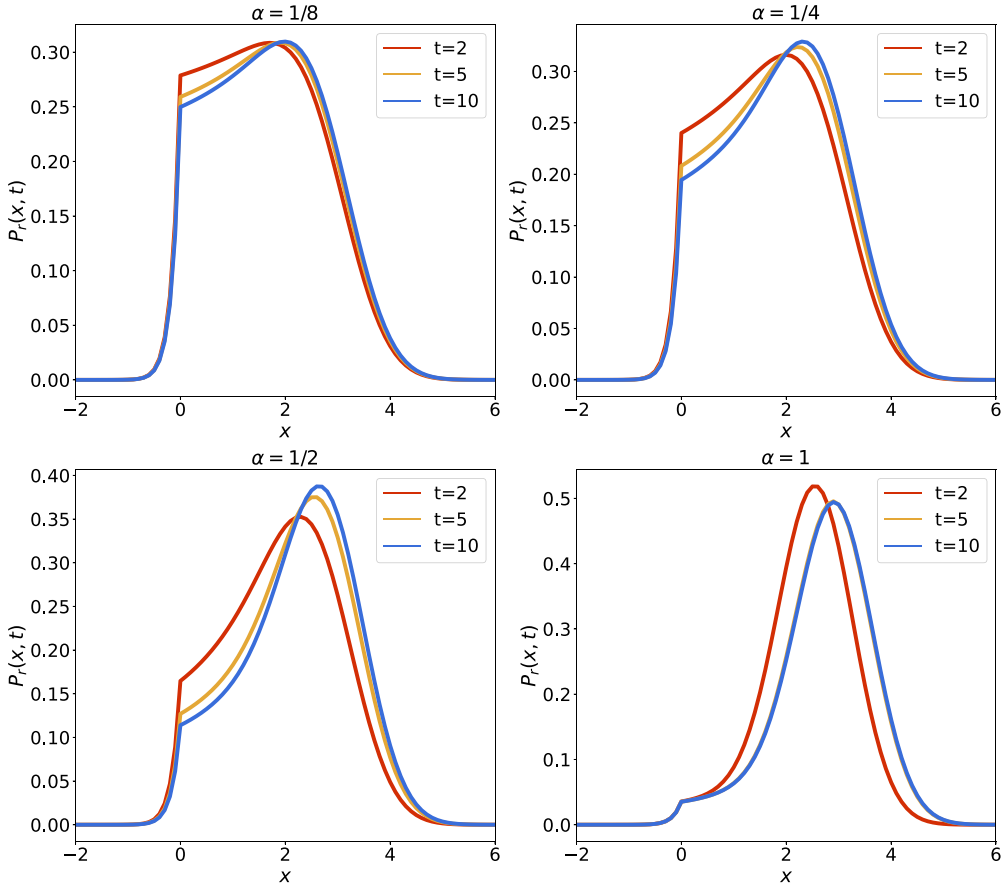

Figure 6. Numerical results for time evolution of the PDFs (50) for the subdiffusive O–U process with resetting, corresponding to process with memory kernel $\eta(t) = \mathrm{e}^{-rt}\frac{t^{\alpha-1}}{\Gamma(\alpha)}$, $0 < \alpha < 1$, $r > 0$. We set $x_0 = 0$, $\mu = 3$, $\sigma = 1$, $\lambda = 1$ and $r = 0.1$.

where we introduce long-tailed waiting times in the random walk model. It results in the presence of a memory function in the Fokker–Planck equation for the generalised O–U process. This model as a special case contains the previously introduced models on O–U processes on two and three dimensional comb-like structures, which are subdiffusive O–U processes with fractional exponent $1/2$ and $1/4$, respectively. The present model can also describe a generalised O–U process under Poissonian resetting of the particle to its initial position if in the Fokker–Planck equation we introduce an exponentially truncated memory kernel. It is shown that due to the resetting the particle approaches a non-equilibrium stationary state in the long time limit. The analytically obtained results are compared with numerical evaluations and simulations and good agreement is shown. The derivation of a general O–U model under different resetting mechanism, such as power-law or sharp resetting in which the time between two restarts is fixed, we leave for a future research. Another interesting model for future research could be the analysis of the corresponding first passage time problem of the generalised O–U process in the presence of resetting and the determination of the optimal search strategy by calculation of the mean first passage time.

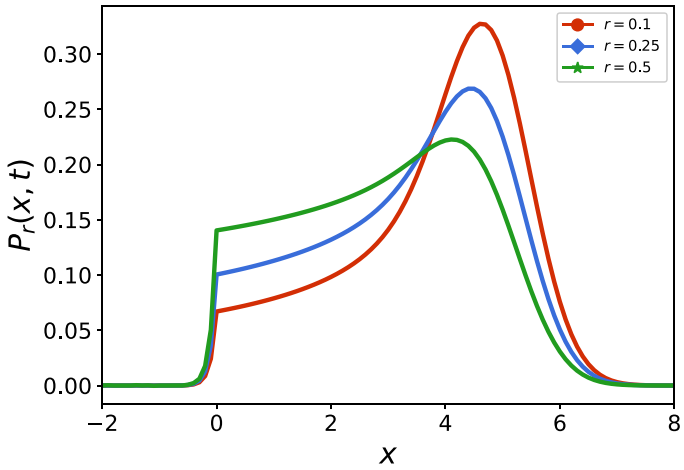

Figure 7. PDF for the time fractional O–U process with resetting, which corresponds to the process with $\eta_r(t) = \mathrm{e}^{-rt}\frac{t^{\alpha-1}}{\Gamma(\alpha)}$, $0<\alpha<1$, $r>0$. We set $x_0=0$, $t=10$, $\mu=5$, $\sigma=1$, $\lambda=1$, $\alpha=0.5$ for different resetting rates r.

Data availability statement

No new data were created or analysed in this study.

Acknowledgments

The Authors acknowledge financial support by the German Science Foundation (DFG, Grant number ME 1535/12-1), and by the Alliance of International Science Organizations (Project No. ANSO-CR-PP-2022-05). TS was supported by the Alexander von Humboldt Foundation. PT, LK and TS acknowledge support from the bilateral Macedonian-Austrian project No. 20-667/10 (WTZ MK03/2024). PT and RM acknowledge support from the Erwin Schrödinger International Institute for Mathematics and Physics in Vienna and TS acknowledges the hospitality and support from the Lorentz Center in Leiden.

Appendix A. Fractional calculus and related Mittag–Leffler functions

The Riemann–Liouville fractional integral of order $\mu>0$ is defined by [72]

$$I^{\mu}_{0+}f(t) = \frac{1}{\Gamma(\mu)}\int_0^t \frac{f(t')}{(t-t')^{1-\mu}}\,\mathrm{d}t', \quad \Re(\mu)>0, \tag{A.1}$$

such that for $\mu=0$ it is

$$I^{0}_{0+}f(t) = f(t)\,. \tag{A.2}$$

The Riemann–Liouville fractional derivative of order $0<\mu<1$ is defined as a derivative of the Riemann–Liouville fractional integral of a function [72],

$${}_{\mathrm{RL}}D^{\mu}_{t}f(t) = \frac{\mathrm{d}}{\mathrm{d}t}I^{1-\mu}_{0+}f(t) = \frac{1}{\Gamma(1-\alpha)}\frac{\mathrm{d}}{\mathrm{d}t}\int_0^t (t-t')^{-\mu}f(t')\,\mathrm{d}t', \tag{A.3}$$

while the Caputo fractional derivative of order $0 < \mu < 1$ is defined as the Riemann–Liouville fractional integral of the first derivative of a function [72],

$$ {}_{\mathrm{C}}D_t^{\mu} f(t) = I_{0+}^{1-\mu} \frac{\mathrm{d}}{\mathrm{d}t} f(t) = \frac{1}{\Gamma(1-\alpha)} \int_0^t (t-t')^{-\mu} \frac{\mathrm{d}}{\mathrm{d}t'} f(t') \, \mathrm{d}t'. \tag{A.4} $$

The tempered Riemann–Liouville fractional derivative of order $0 < \mu < 1$ with tempering parameter r is defined by [71, 73]

$$ {}_{\mathrm{TRL}}D_{0+}^{\mu} f(t) = \frac{1}{\Gamma(1-\mu)} \frac{\mathrm{d}}{\mathrm{d}t} \int_0^t \mathrm{e}^{-r(t-t')} (t-t')^{-\mu} f(t') \, \mathrm{d}t'. \tag{A.5} $$

The three parameter Mittag–Leffler function (also known as a Prabhakar function) is defined by [74]

$$ E_{\alpha,\beta}^{\gamma}(z) = \sum_{k=0}^{\infty} \frac{(\gamma)_k}{\Gamma(\alpha k + \beta)} \frac{z^k}{k!}, \tag{A.6} $$

where $\beta, \gamma, z \in \mathbb{C}$, $\Re(\alpha) > 0$, $(\gamma)_k$ is the Pochhammer symbol

$$ (\gamma)_0 = 1, \quad (\gamma)_k = \frac{\Gamma(\gamma + k)}{\Gamma(\gamma)}. \tag{A.7} $$

It is a generalisation of the two parameter Mittag–Leffler function (also called generalised Mittag–Leffler function in [75])

$$ E_{\alpha,\beta}^{1}(z) = \sum_{k=0}^{\infty} \frac{z^k}{\Gamma(\alpha k + \beta)} = E_{\alpha,\beta}(z), \tag{A.8} $$

and the one parameter Mittag–Leffler function [75]

$$ E_{\alpha,1}^{1}(z) = \sum_{k=0}^{\infty} \frac{z^k}{\Gamma(\alpha k + 1)} = E_{\alpha}(z). \tag{A.9} $$

The Laplace transform of the three parameter Mittag–Leffler function is given by

$$ \mathcal{L}\left[t^{\beta-1} E_{\alpha,\beta}^{\gamma}(\mp \lambda t^{\alpha}) \right] = \frac{s^{\alpha\gamma-\beta}}{(s^{\alpha} \pm \lambda)^{\gamma}}, \tag{A.10} $$

where $|\lambda / s^{\alpha}| < 1$.

The asymptotic behaviour for large z of the three parameter Mittag–Leffler function can be found from the following expression [76]

$$E^{\gamma}_{\alpha,\beta}(-z) = \frac{z^{-\gamma}}{\Gamma(\gamma)} \sum_{n=0}^{\infty} \frac{\Gamma(\gamma+n)}{\Gamma(\beta-\alpha(\gamma+n))} \frac{(-z)^{-n}}{n!}, \quad z>1, \tag{A.11}$$

i.e.

$$E^{\gamma}_{\alpha,\beta}(-z) \sim \frac{z^{-\gamma}}{\Gamma(\beta-\alpha\gamma)} - \gamma \frac{z^{-(\gamma+1)}}{\Gamma(\beta-\alpha(\gamma+1))}, \quad z \gg 1. \tag{A.12}$$

The multinomial Mittag–Leffler function is defined by [77]

$$E_{(\alpha_1,\alpha_2,\ldots,\alpha_n),\beta}(z_1,z_2,\ldots,z_n) = \sum_{k=0}^{\infty} \sum_{l_1\geq 0, l_2\geq 0,\ldots,l_n\geq 0}^{l_1+l_2+\cdots+l_n=k} \binom{k}{l_1,\ldots,l_n} \frac{\prod_{i=1}^{n} z_i^{l_i}}{\Gamma\left(\beta+\sum_{i=1}^{n}\alpha_i l_i\right)}, \tag{A.13}$$

where

$$\binom{k}{l_1,\ldots,l_n} = \frac{k!}{l_1!l_2!\ldots l_n!},$$

are the multinomial coefficients. Its Laplace transform reads

$$\mathcal{L}\left[t^{\beta-1} E_{(\alpha_1,\alpha_2,\ldots,\alpha_n),\beta}(\mp\lambda_1 t^{\alpha_1}, \mp\lambda_2 t^{\alpha_2},\ldots,\mp\lambda_n t^{\alpha_n})\right] = \frac{s^{-\beta}}{1\pm\sum_{j=1}^{n}\lambda_j s^{-\alpha_j}}. \tag{A.14}$$

Appendix B. Tauberian theorems

The asymptotic behaviour of a given function $r(t)$ can be analysed by means of the Tauberian theorems [36]. One of the theorems states that if the asymptotic behaviour of $r(t)$ for $t\to\infty$ is given by

$$r(t) \sim t^{-\alpha}, \quad t\to\infty, \quad \alpha>0, \tag{B.1}$$

then, the corresponding Laplace pair $\hat{r}(s) = \mathcal{L}[r(t)]$ has the following behaviour for $s\to 0$

$$\hat{r}(s) \sim \Gamma(1-\alpha)\, s^{\alpha-1}, \quad s\to 0. \tag{B.2}$$

The theorem also works in the opposite direction, ensuring that $r(t)$ is the non-negative and monotone function at infinity.

This theorem can be formulated in the form of the so-called Hardy–Littlewood theorem. The theorem states that, if the Laplace–Stieltjes transform of a given non-decreasing function F with $F(0)=0$, defined by Stieltjes integral

$$\omega(s) = \int_0^{\infty} \mathrm{e}^{-st}\, \mathrm{d}F(t), \tag{B.3}$$

has asymptotic behaviour

$$\omega(s) \sim Cs^{-\nu}, \quad s \to \infty \quad (s \to 0), \tag{B.4}$$

where $\nu \geq 0$ and C are real numbers, then the function F has asymptotic behaviour

$$F(t) \sim \frac{C}{\Gamma(\nu+1)} t^{\nu}, \quad t \to 0 \quad (t \to \infty). \tag{B.5}$$

Appendix C. Mixed subdiffusive O–U processes

Here we observe the mixed subdiffusive processes with different power-law memory functions. This case can be represented by the memory kernel $\eta(t) = \omega_1 \frac{t^{\alpha_1-1}}{\Gamma(\alpha_1)} + \omega_2 \frac{t^{\alpha_2-1}}{\Gamma(\alpha_2)}$, where $0 < \alpha_1 < \alpha_2 < 1, \omega_1 + \omega_2 = 1$ and $\hat{\eta}(s) = \omega_1 s^{-\alpha_1} + \omega_2 s^{-\alpha_2}$. We note that for $\alpha_1 \equiv \alpha$ and $\alpha_2 \equiv 1$, we have a combination of standard diffusive and subdiffusive motion. The Fokker–Planck equation for this mixed motion becomes

$$\begin{aligned} \frac{\partial}{\partial t} P(x,t) = \frac{\mathrm{d}}{\mathrm{d}t} \int_0^t \left[\omega_1 \frac{(t-t')^{\alpha_1-1}}{\Gamma(\alpha_1)} + \omega_2 \frac{(t-t')^{\alpha_2-1}}{\Gamma(\alpha_2)} \right] \\ \times \left\{ \lambda \frac{\partial}{\partial x} \left[(x-\mu) P(x,t') \right] + \frac{\sigma^2}{2} \frac{\partial^2}{\partial x^2} P(x,t') \right\} \mathrm{d}t'. \end{aligned} \tag{C.1}$$

From the general results for the mean value (18), we can directly obtain the mean value for the mixed subdiffusive O–U processes in Laplace space. Thus, we have

$$\langle \hat{x}(s) \rangle = x_0 \frac{s^{-1}}{1 + \lambda(\omega_1 s^{-\alpha_1} + \omega_2 s^{-\alpha_2})} + \lambda\mu \frac{(\omega_1 s^{-\alpha_1} + \omega_2 s^{-\alpha_2}) s^{-1}}{1 + \lambda(\omega_1 s^{-\alpha_1} + \omega_2 s^{-\alpha_2})}, \tag{C.2}$$

from which by inverse Laplace transform, we find the exact result in terms of Mittag–Leffler functions,

$$\begin{aligned} \langle x(t) \rangle_{\mathrm{g}} = x_0 \sum_{k=0}^{\infty} (-\lambda\omega_2)^k t^{\alpha_2 k} E^{k+1}_{\alpha_1, \alpha_2 k+1}(-\lambda\omega_1 t^{\alpha_1}) \\ + \sum_{k=0}^{\infty} \Big\{ \lambda\mu\omega_1 (-\lambda\omega_2)^k t^{\alpha_2 k + \alpha_1} E^{k+1}_{\alpha_1, \alpha_2 k + \alpha_1 + 1}(-\lambda\omega_1 t^{\alpha_1}) \\ + \lambda\mu\omega_2 (-\lambda\omega_2)^k t^{\alpha_2 k + \alpha_2} E^{k+1}_{\alpha_1, \alpha_2 k + \alpha_2 + 1}(-\lambda\omega_1 t^{\alpha_1}) \Big\}. \end{aligned} \tag{C.3}$$

By asymptotic analysis, employing Tauberian theorems (see appendix B), we find that the mean value in the long time limit behaves as

$$\begin{aligned} \langle x(t) \rangle_{\mathrm{g}} \sim \frac{x_0}{\lambda\omega_2} \left[\frac{t^{-\alpha_2}}{\Gamma(1-\alpha_2)} - \frac{\omega_1}{\omega_2} \frac{t^{-(2\alpha_2-\alpha_1)}}{\Gamma(1-[2\alpha_2-\alpha_1])} \right] \\ + \mu \frac{\omega_1}{\omega_2} \left[\frac{t^{-(\alpha_2-\alpha_1)}}{\Gamma(1-[\alpha_2-\alpha_1])} - \frac{\omega_1}{\omega_2} \frac{t^{-2(\alpha_2-\alpha_1)}}{\Gamma(1-2[\alpha_2-\alpha_1])} \right] \\ + \mu \left[1 - \frac{\omega_1}{\omega_2} \frac{t^{-(\alpha_2-\alpha_1)}}{\Gamma(1-[\alpha_2-\alpha_1])} \right], \end{aligned} \tag{C.4}$$

i.e. it reaches the mean μ. Correspondingly, for the MSD from the general results (19), we find in Laplace space

$$\begin{aligned}\langle \hat{x}^2(s)\rangle = x_0^2 \frac{s^{-1}}{1+2\lambda\left(\omega_1 s^{-\alpha_1}+\omega_2 s^{-\alpha_2}\right)} + \sigma^2 \frac{s^{-1}\left(\omega_1 s^{-\alpha_1}+\omega_2 s^{-\alpha_2}\right)}{1+2\lambda\left(\omega_1 s^{-\alpha_1}+\omega_2 s^{-\alpha_2}\right)} \\ + 2\lambda\mu x_0 \frac{\left(\omega_1 s^{-\alpha_1}+\omega_2 s^{-\alpha_2}\right)s^{-1}}{\left(1+2\lambda\left(\omega_1 s^{-\alpha_1}+\omega_2 s^{-\alpha_2}\right)\right)\left(1+\lambda\left(\omega_1 s^{-\alpha_1}+\omega_2 s^{-\alpha_2}\right)\right)} \\ + 2\lambda^2\mu^2 \frac{\left(\omega_1 s^{-\alpha_1}+\omega_2 s^{-\alpha_2}\right)^2 s^{-1}}{\left(1+2\lambda\left(\omega_1 s^{-\alpha_1}+\omega_2 s^{-\alpha_2}\right)\right)\left(1+\lambda\left(\omega_1 s^{-\alpha_1}+\omega_2 s^{-\alpha_2}\right)\right)},\end{aligned} \tag{C.5}$$

which by inverse Laplace transform leads to

$$\begin{aligned}\langle x^2(t)\rangle = x_0^2 \sum_{k=0}^{\infty} (-2\lambda\omega_2)^k t^{\alpha_2 k} E^{k+1}_{\alpha_1,\alpha_2 k+1}\left(-2\lambda\omega_1 t^{\alpha_1}\right) \\ + \sum_{k=0}^{\infty}\left\{\sigma^2(-2\lambda\omega_2)^k\left[\omega_1 t^{\alpha_2 k+\alpha_1} E^{k+1}_{\alpha_1,\alpha_2 k+\alpha_1+1}\left(-2\lambda\omega_1 t^{\alpha_1}\right) + \omega_2 t^{\alpha_2 k+\alpha_2} E^{k+1}_{\alpha_1,\alpha_2 k+\alpha_2+1}\left(-2\lambda\omega_1 t^{\alpha_1}\right)\right]\right\} \\ + 2\lambda\mu\omega_2 x_0 t E_{(\alpha,1,2\alpha,2,\alpha+1),2}\left(-3\lambda\omega_1 t^{\alpha}, -3\lambda\omega_2 t, -2\lambda^2\omega_1^2 t^{2\alpha}, -2\lambda^2\omega_2^2 t^2, -4\lambda^2\omega_1\omega_2 t^{\alpha+1}\right) \\ + 2\lambda\mu\omega_1 x_0 t^{\alpha_1} \\ \times E_{(\alpha_1,\alpha_2,\alpha_1+\alpha_2,2\alpha_1,2\alpha_2),\alpha_2+1}\left(-3\lambda\omega_1 t^{\alpha_1}, -3\lambda\omega_2 t^{\alpha_2}, -4\lambda^2\omega_1\omega_2 t^{\alpha_1+\alpha_2}, -2\lambda^2\omega_1^2 t^{2\alpha_1}, -2\lambda^2\omega_2^2 t^{2\alpha_2}\right) \\ + 2\lambda^2\mu^2\omega_1^2 t^{2\alpha_1} \\ \times E_{(\alpha_1,\alpha_2,\alpha_1+\alpha_2,2\alpha_1,2\alpha_2),2\alpha_1+1}\left(-3\lambda\omega_1 t^{\alpha_1}, -3\lambda\omega_2 t^{\alpha_2}, -4\lambda^2\omega_1\omega_2 t^{\alpha_1+\alpha_2}, -2\lambda^2\omega_1^2 t^{2\alpha_1}, -2\lambda^2\omega_2^2 t^{2\alpha_2}\right) \\ + 2\lambda^2\mu^2\omega_2^2 t^{2\alpha_2} \\ \times E_{(\alpha_1,\alpha_2,\alpha_1+\alpha_2,2\alpha_1,2\alpha_2),2\alpha_2+1}\left(-3\lambda\omega_1 t^{\alpha_1}, -3\lambda\omega_2 t^{\alpha_2}, -4\lambda^2\omega_1\omega_2 t^{\alpha_1+\alpha_2}, -2\lambda^2\omega_1^2 t^{2\alpha_1}, -2\lambda^2\omega_2^2 t^{2\alpha_2}\right) \\ + 4\lambda^2\mu^2\omega_1\omega_2 t^{\alpha_1+\alpha_2} \\ \times E_{(\alpha_1,\alpha_2,\alpha_1+\alpha_2,2\alpha_1,2\alpha_2),\alpha_1+\alpha_2+1}\left(-3\lambda\omega_1 t^{\alpha_1}, -3\lambda\omega_2 t^{\alpha_2}, -4\lambda^2\omega_1\omega_2 t^{\alpha_1+\alpha_2}, -2\lambda^2\omega_1^2 t^{2\alpha_1}, -2\lambda^2\omega_2^2 t^{2\alpha_2}\right).\end{aligned} \tag{C.6}$$

By using the Tauberian theorems, we find the asymptotic behaviour of the MSD in the long time limit,

$$\begin{aligned}\langle x^2(t)\rangle_{\mathrm{g}} \sim \frac{x_0^2}{2\lambda\omega_2}\left[\frac{t^{-\alpha_2}}{\Gamma(1-\alpha_2)} + \frac{\omega_1}{\omega_2}\frac{t^{-(2\alpha_2-\alpha_1)}}{\Gamma(1-[2\alpha_2-\alpha_1])}\right] + \frac{\sigma^2}{2\lambda}\left[1 - \frac{\omega_1^2}{\omega_2^2}\frac{t^{-2(\alpha_2-\alpha_1)}}{\Gamma(1-2[\alpha_2-\alpha_1])}\right] \\ + \frac{\mu x_0}{\lambda\omega_2}\left[\frac{t^{-\alpha_2}}{\Gamma(1-\alpha_2)} - \frac{\omega_1}{\omega_2}\frac{t^{-(2\alpha_2-\alpha_1)}}{\Gamma(1-[2\alpha_2-\alpha_1])} - 2\frac{\omega_1^2}{\omega_2^2}\frac{t^{-(3\alpha_2-2\alpha_1)}}{\Gamma(1-[3\alpha_2-2\alpha_1])}\right] \\ + \mu^2\left[1 - 3\frac{\omega_1^2}{\omega_2^2}\frac{t^{-2(\alpha_2-\alpha_1)}}{\Gamma(1-2[\alpha_2-\alpha_1])} - 3\frac{\omega_1^3}{\omega_2^3}\frac{t^{-3(\alpha_2-\alpha_1)}}{\Gamma(1-3[\alpha_2-\alpha_1])}\right].\end{aligned} \tag{C.7}$$

From here we conclude that in the long time limit the MSD approaches to the thermal equilibrium $\langle x_{\mathrm{th}}^2\rangle = \frac{\sigma^2}{2\lambda} + \mu^2$.

Graphical representation of the MSD (C.6) for different values of system's parameters in case of mixed subdiffusive and combined standard and subdiffusive processes is given in figure C1.

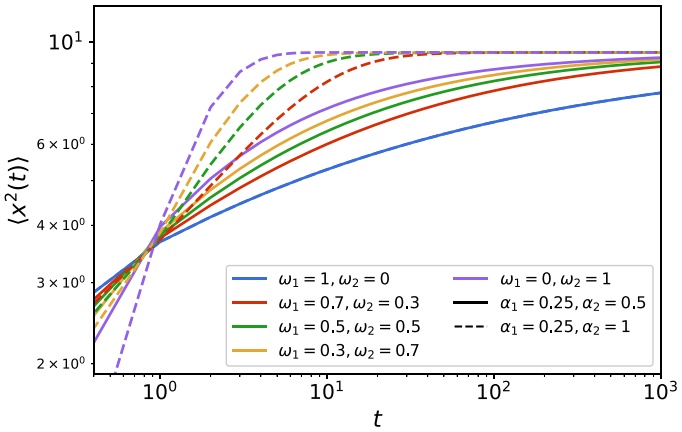

Figure C1. MSD (C.6) for mixed subdiffusive O–U process and combined standard and subdiffusive O–U processes ()$< \alpha_1 < 1$, $\alpha_2 = 1$). We set $x_0 = 0$, $\mu = 3$ $\sigma = 1$ and $\lambda = 1$.

Appendix D. Error analysis of the numerical method in section 3.2

In order to analyse the precision of the method used in this paper, section 3.2, for simulating the processes, we calculate the error between the numerical results of the PDFs acquired by numerically solving the Fokker–Planck equation (26) and the PDFs of the simulations. Of great interest is to see how the precision of the simulations as a function of the number of trajectories N and the size of the time step Δt. To do that we introduce the following expression

$$R_k = \frac{|P_{s,k}(x,t) - P_{n,k}(x,t)|}{P_{n,k}(x,t)}, \tag{D.1}$$

the relative error defining the ratio of the absolute error of a measurement to the measurement being taken, where $P_n(x,t)$ is the numerically calculated value and, $P_s(x,t)$ is the experimental or the simulated value. By averaging over all of the sample points N, the average relative error is calculated,

$$\langle R\rangle = \frac{\sum_{k=0}^{N} R_k}{N}. \tag{D.2}$$

A convenient equation for determining the precision or the error of the simulations is the standard deviation, given by

$$S = \sqrt{\frac{\sum_{k=0}^{N} d_k}{N-1}}, \tag{D.3}$$

where

$$d_k = (R_k - \langle R\rangle)^2. \tag{D.4}$$

In figure D1 we present the standard deviation (D.3) as a function of the number of trajectories used for simulating the PDFs. It is clearly evident that the increase in the number of trajectories results in more precise simulations. At first we have a very fast increase in the

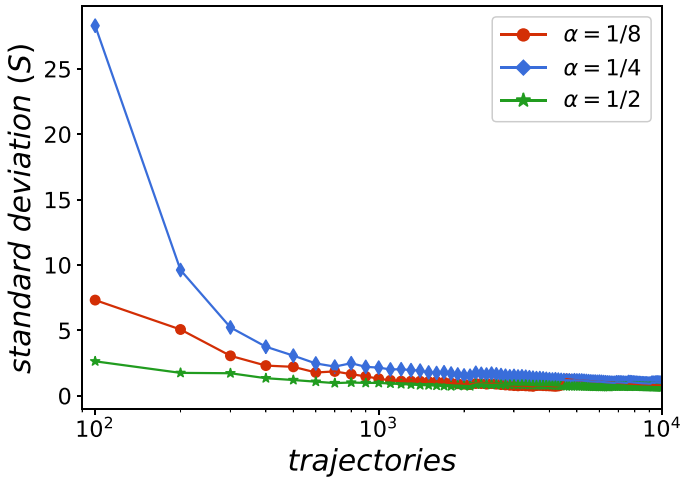

Figure D1. Standard error analysis between the numerically calculated values of the PDFs and simulations with different number of trajectories. Parameters: $x_0 = 0$, $\mu = 2$, $\sigma = 1$, $\lambda = 1$, $t = 10^4$, $\mathrm{d}t = 0.1$, $\mathrm{d}s = 0.01$.

precision for the first few thousands of trajectories and after that roughly a linear decrease in the standard deviation and increase in the precision of the simulations. Further increase in the sample of trajectories will always improve the simulations, but at the cost of time and computational power, so choosing the number of sample trajectories which will allow balance between satisfactory precision of the results and reduced computational time and power is essential in this case.

ORCID iDs

P Trajanovski https://orcid.org/0000-0001-7574-183X
P Jolakoski https://orcid.org/0000-0001-7384-8756
R Metzler https://orcid.org/0000-0002-6013-7020
T Sandev https://orcid.org/0000-0001-9120-3847

References

[1] Brown R 1828 A brief account of microscopical observations on the particles contained in the pollen of plants and on the general existence of active molecules in organic and inorganic bodies *Phil. Mag.* **4** 161
[2] Einstein A 1905 Über die von der molekularkinetischen Theorie der Wärme geforderte Bewegung von in ruhenden Flüssigkeiten suspendierten Teilchen *Ann. Phys.* **322** 549
[3] Smoluchowski M 1906 Zur kinetischen Theorie der Brownschen Molekularbewegung und der Suspensionen *Ann. Phys.* **326** 756
[4] Ornstein L S 1919 On the Brownian Motion *Proc. Acad. Amst.* **21** 96
[5] Uhlenbeck G E and Ornstein L S 1930 On the theory of Brownian motion *Phys. Rev.* **36** 823
[6] Cáceres M O and Budini A A 1997 The generalized Ornstein-Uhlenbeck process *J. Phys. A: Math. Gen.* **30** 8427
[7] Bezuglyy V and Mehlig B 2006 Generalized Ornstein-Uhlenbeck processes *J. Math. Phys.* **47** 073301

[8] Metzler R, Barkai E and Klafter J 1999 Anomalous diffusion and relaxation close to thermal equilibrium: a fractional Fokker-Planck equation approach *Phys. Rev. Lett.* **82** 3563
[9] Metzler R and Klafter J 2000 The random walk's guide to anomalous diffusion: a fractional dynamics approach *Phys. Rep.* **339** 1
[10] Eliazar I and Klafter J 2009 From Ornstein-Uhlenbeck dynamics to long-memory processes and fractional Brownian motion *Phys. Rev.* E **79** 021115
[11] Oxley W and Kim E J 2018 Scalings and fractals in information geometry: Ornstein-Uhlenbeck processes *J. Stat. Mech.* **2018** 113401
[12] Le Vot F, Yuste S B and Abad E 2019 Standard and fractional Ornstein-Uhlenbeck process on a growing domain *Phys. Rev.* E **100** 012142
[13] Mardoukhi Y, Chechkin A and Metzler R 2020 Spurious ergodicity breaking in normal and fractional Ornstein-Uhlenbeck process *New J. Phys.* **22** 073012
[14] Chevillard L 2017 Regularized fractional Ornstein-Uhlenbeck processes and their relevance to the modeling of fluid turbulence *Phys. Rev.* E **96** 033111
[15] Shao Y 1995 The fractional Ornstein-Uhlenbeck process as a representation of homogeneous Eulerian velocity turbulence *Physica* D **83** 461
[16] Maller R A, Müller G, Szimayer A and Andersen T G 2009 Ornstein–Uhlenbeck Processes and Extensions *Handbook of Financial Time Series* ed T Mikosch, J -P Kreiß and R A Davis (Springer) pp 421–37
[17] Fyodorov Y V, Khoruzhenko B A and Simm N J 2016 Fractional Brownian motion with hurst index $H = 0$ and the Gaussian unitary ensemble *Ann. Prob.* **44** 2980
[18] Norregaard K, Metzler R, Ritter C M, Berg-Sørensen K and Oddershede L B 2017 Manipulation and motion of organelles and single molecules in living cells *Chem. Rev.* **117** 4342
[19] Mardoukhi Y, Jeon J-H, Chechkin A and Metzler R 2018 Fluctuations of random walks in critical random environments *Phys. Chem. Chem. Phys.* **20** 20427
[20] Vasicek O 1977 An equilibrium characterization of the term structure *J. Financ. Econom.* **5** 177
[21] Ricciardi L M and Sacerdote L 1979 The Ornstein-Uhlenbeck process as a model for neuronal activity: I. Mean and variance of the firing time *Biol. Cybern.* **35** 1–9
[22] Meylahn J M, Sabhapandit S and Touchette H 2015 Large deviations for Markov processes with resetting *Phys. Rev.* E **92** 062148
[23] Pal A 2015 Diffusion in a potential landscape with stochastic resetting *Phys. Rev.* E **91** 012113
[24] Singh P and Pal A 2021 Extremal statistics for stochastic resetting systems *Phys. Rev.* E **103** 052119
[25] Smith N R 2022 Anomalous scaling and first-order dynamical phase transition in large deviations of the Ornstein-Uhlenbeck process *Phys. Rev.* E **105** 014120
[26] Smith N R and Majumdar S N 2022 Condensation transition in large deviations of self-similar Gaussian processes with stochastic resetting *J. Stat. Mech.* 053212
[27] Goerlich R, Li M, Albert S, Manfredi G, Hervieux P-A and Genet C 2021 Noise and ergodic properties of Brownian motion in an optical tweezer: Looking at regime crossovers in an Ornstein-Uhlenbeck process *Phys. Rev.* E **103** 032132
[28] Trajanovski P, Jolakoski P, Zelenkovski K, Iomin A, Kocarev L and Sandev T 2023 Ornstein-Uhlenbeck process and generalizations: particle dynamics under comb constraints and stochastic resetting *Phys. Rev.* E **107** 054129
[29] Trajanovski P, Jolakoski P, Kocarev L and Sandev T 2023 Ornstein-Uhlenbeck process on three-dimensional comb under stochastic resetting *Mathematics* **11** 3576
[30] Doob J L 1942 The Brownian movement and stochastic equations *Ann. Math.* **43** 351
[31] Risken H 1996 *The Fokker-Planck equation: Methods of Solution and Applications* (Springer)
[32] Montroll E W and Weiss G H 1965 Random walks on lattices *J. Math. Phys.* **II** 167
[33] Hughes B D 1996 *Random Walks and Random Environments* (Oxford University Press)
[34] Sokolov I M and Klafter J 2005 From diffusion to anomalous diffusion: a century after Einstein's Brownian motion *Chaos* **15** 026103
[35] Fogedby H C 1994 Langevin equations for continuous time Lévy flights *Phys. Rev.* E **50** 1657
[36] Feller W 1991 *An Introduction to Probability Theory and its Applications* vol 2 (Willey)
[37] Saichev A I and Zaslavsky G M 1997 Fractional kinetic equations: solutions and applications *Chaos* **7** 753
[38] Barkai E and Silbey R J 2000 Fractional Kramers equation *J. Phys. Chem.* B **104** 3866
[39] Chechkin A and Sokolov I M 2021 Relation between generalized diffusion equations and subordination schemes *Phys. Rev.* E **103** 032133

[40] Piryatinska A, Saichev A I and Woyczynski W A 2005 Models of anomalous diffusion: the subdiffusive case *Physica* A **349** 375
[41] Magdziarz M and Weron K 2006 Anomalous diffusion schemes underlying the Cole-Cole relaxation: the role of the inverse-time α-stable subordinator *Physica* A **367** 1–6
[42] Magdziarz M, Weron A and Klafter J 2008 Equivalence of the fractional Fokker-Planck and subordinated Langevin equations: the case of a time-dependent force *Phys. Rev. Lett.* **101** 210601
[43] Baule A and Friedrich R 2005 Joint probability distributions for a class of non-Markovian processes *Phys. Rev.* E **71** 26101
[44] Baule A and Friedrich R 2007 A fractional diffusion equation for two-point probability distributions of a continuous-time random walk *Europhys. Lett.* **77** 10002
[45] Kleinhans D and Friedrich R 2007 Continuous-time random walks: simulation of continuous trajectories *Phys. Rev.* E **76** 061102
[46] Sandev T, Metzler R and Chechkin A 2018 From continuous time random walks to the generalized diffusion equation *Fract. Calc. Appl. Anal.* **21** 10
[47] Sandev T, Sokolov I M, Metzler R and Chechkin A 2017 Beyond monofractional kinetics *Chaos Solitons Fractals* **102** 210
[48] Orzel S, Mydlarczyk W and Jurlewicz A 2013 Accelerating subdiffusions governed by multiple-order time-fractional diffusion equations: Stochastic representation by a subordinated Brownian motion and computer simulations *Phys. Rev.* E **87** 032110
[49] Stanislavsky A, Weron K and Weron A 2014 Anomalous diffusion with transient subordinators: a link to compound relaxation laws *J. Chem. Phys.* **140** 054113
[50] Metzler R and Klafter J 2000 The Random Walk's guide to anomalous diffusion: a fractional dynamics approach *Phys. Rep.* **339** 1–77
[51] Magdziarz M 2009 Black-Scholes formula in subdiffusive regime *J. Stat. Phys.* **136** 553–64
[52] Barkai E 2001 Fractional Fokker-Planck equation, solution and application *Phys. Rev.* E **63** 046118
[53] Meerschaert M M, Benson D A, Scheffler H-P and Baeumer B 2002 Stochastic solution of space-time fractional diffusion equations *Phys. Rev.* E **65** 041103
[54] Bazhlekova E and Bazhlekov I 2019 Subordination Approach to Space-Time Fractional Diffusion *Mathematics* **7** 415
[55] Sandev T, Chechkin A, Kantz H and Metzler R 2015 Diffusion and Fokker-Planck-Smoluchowski equations with generalized memory kernel *Fract. Calc. Appl. Anal.* **18** 1006
[56] Domazetoski V, Masó-Puigdellosas A, Sandev T, Méndez V, Iomin A and Kocarev L 2020 Stochastic resetting on comblike structures *Phys. Rev. Res.* **2** 033027
[57] Sandev T, Domazetoski V, Iomin A and Kocarev L 2021 Diffusion-advection equations on a comb: Resetting and random search *Mathematics* **9** 221
[58] Méndez V, Iomin A, Horsthemke W and Campos D 2017 Langevin dynamics for ramified structures *J. Stat. Mech.* 063205
[59] Ribeiro H V, Tateishi A A, Alves L G A, Zola R S and Lenzi E K 2014 Investigating the interplay between mechanisms of anomalous diffusion via fractional Brownian walks on a comb-like structure *New J. Phys.* **16** 093050
[60] Abate J and Valkó P P 2004 Multi-precision Laplace transform inversion *Int. J. Numer. Methods Eng.* **60** 979
[61] Valkó P P and Abate J 2004 Comparison of sequence accelerators for the Gaver method of numerical Laplace transform inversion *Comput. Math. Appl.* **48** 629
[62] Carnaffan S and Kawai R 2017 Solving multidimensional fractional Fokker-Planck equations via unbiased density formulas for anomalous diffusion processes *J. Sci. Comput.* **39** 5
[63] Kawai R 2024 Unbiased density computation for stochastic resetting *J. Phys. A: Math. Theor.* **57** 295002
[64] Evans M R, Majumdar S N and Schehr G 2020 Stochastic resetting and applications *J. Phys. A: Math. Theor.* **53** 193001
[65] Evans M R and Majumdar S N 2014 Diffusion with resetting in arbitrary spatial dimension *J. Phys. A: Math. Theor.* **47** 285001
[66] Masó-Puigdellosas A, Campos D and Méndez V 2019 Transport properties and first-arrival statistics of random motion with stochastic reset times *Phys. Rev.* E **99** 012141
[67] Bodrova A S, Chechkin A V and Sokolov I M 2019 Scaled Brownian motion with renewal resetting *Phys. Rev.* E **100** 012120
Bodrova A S and Sokolov I M 2020 Resetting processes with noninstantaneous return *Phys. Rev.* E **101** 052130

[68] Evans M R and Majumdar S N 2011 Diffusion with stochastic resetting *Phys. Rev. Lett.* **106** 160601
[69] Sandev T and Iomin A 2022 *Special Functions of Fractional Calculus: Applications to Diffusion and Random Search Processes* (World Scientific)
[70] Prudnikov A P, Bryckov J A and Maricev O I 2003 *Integrals and Series* (*More Special Functions*) vol 3 (Gordon and Breach)
[71] Sandev T 2017 Generalized Langevin equation and the Prabhakar derivative *Mathematics* **5** 66
[72] Prabhakar T R 1971 A singular integral equation with a generalized Mittag Leffler function in the kernel *Yokohama Math. J.* **19** 7–15
[73] Erdelyi A, Magnus W, Oberhettinger F and Tricomi F G 1955 *Higher Transcedental Functions* vol 3 (McGraw-Hill)
[74] Prabhakar T R 1971 A singular integral equation with a generalized Mittag Leffler function in the kernel *Yokohama Math. J.* **19** 7
[75] Erdelyi A, Magnus W, Oberhettinger F and Tricomi F G 1955 *Higher Transcedental Functions* vol 3 (McGraw-Hill)
[76] Garra R and Garrappa R 2018 The Prabhakar or three parameter Mittag-Leffler function: theory and application *Commun. Nonlin. Sci. Numer. Simul.* **56** 314
[77] Luchko Y and Gorenflo R 1999 An operational method for solving fractional differential equations with the Caputo derivatives *Acta Math. Vietnam.* **24** 207–33
Hilfer R, Luchko Y and Tomovski Z 2009 Operational method for the solution of fractional differential equations with generalized Riemann-Liouville fractional derivatives *Fract. Calc. Appl. Anal.* 299